Mater. Res. Soc. Symp. Proc. Vol. 924 © 2006 Materials Research Society 0924-Z03-02

Size-Related Plasticity Effects in AFM Silicon Cantilever Tips*

Malgorzata Kopycinska-Mueller, Roy H. Geiss, and Donna C. Hurley
Materials Reliability Division, National Institute of Standards and Technology, 325 Broadway, Boulder, Colorado, 80305

ABSTRACT

We are developing dynamic atomic force microscopy (AFM) techniques to determine nanoscale elastic properties. Atomic force acoustic microscopy (AFAM) makes use of the resonant frequencies of an AFM cantilever while its tip contacts the sample surface at a given static load. Our methods involve nanosized silicon probes with tip radius R ranging from approximately 10 nm to 150 nm. The resulting radius of contact between the tip and the sample is less than 20 nm. However, the contact stress can be greater than a few tens of gigapascals, exceeding the theoretical yield strength of silicon by a factor of two to four. Our AFAM experiments indicate that, contrary to expectation, tips can sometimes withstand such stresses without fracture. We subjected ten tips to the same sequence of AFAM experiments. Each tip was brought into contact with a fused quartz sample at different static loads. The load was systematically increased from about 0.4 μN to 6 μN. Changes in tip geometry were observed in images acquired in a scanning electron microscope (SEM) between the individual AFAM experiments. All of the tips with $R <$ 10 nm broke during the first AFAM experiments at static loads less than 1.6 μN. Tips with $R >$ 40 nm plastically deformed under such loads. However, a group of tips with R from 25 nm to 30 nm neither broke nor deformed during the tests. In order to reach higher contact stresses, two additional tips with similar values of R were used in identical experiments on nickel and sapphire samples. Although the estimated stresses exceeded 40 GPa, we did not observe any tip fracture events. Our qualitative observations agree with more systematic studies performed by other groups on various nanostructures. The results emphasize the necessity of understanding the mechanics of nanometer-scaled bodies and the impact of size effects on measurements of mechanical properties on such scales.

INTRODUCTION

Atomic force acoustic microscopy (AFAM) is one of the so-called ultrasonic atomic force microscopy (AFM) methods [1-3] that are able to probe material elastic properties with unprecedented lateral and depth resolution. AFAM is a contact-mode technique that uses the resonant frequencies of an AFM cantilever in the range from approximately 0.1 MHz to 3 MHz to determine a sample's elastic properties from the tip-sample contact stiffness k^* [3]. AFAM employs commercially available micromachined rectangular cantilevers of single-crystal silicon with sharp sensor tips. The rectangular shape simplifies the modeling of the cantilever's dynamic behavior, required for calculations of the tip-sample contact stiffness.

Because the AFM tips often have a radius of curvature $R <$ 10 nm, the resulting radius of tip-sample contact a is typically less than a few nanometers. AFAM probes the elastic properties of the sample to a depth of about three times the contact radius [4]. Therefore,

in order to ensure that the tip probes the properties of the sample and not merely that of the contamination layers, relatively high static loads F (~ 0.4 μN to 3 μN) must be applied. However, such small a and large F result in very large stresses – from several gigapascals to a few tens of gigapascals – which can be several times greater than the predicted yield strength of silicon [5]. Due to the large stresses applied in contact, the silicon AFM tips wear. Here, we use the term "wear" to mean changes in the tip shape (such as an increase in R), plastic deformation and fracture. In our experience, coating the tips with layers of hard materials such as silicon nitride or polycrystalline diamond does not prevent tip wear because the coating often delaminates.

In this study, we performed systematic AFAM and SEM experiments to better understand tip wear processes and their impact on measurement performance. To achieve this, we subjected several AFM tips to the same set of AFAM experiments. The values of contact stiffness obtained from the AFAM tests were used to calculate tip-sample contact parameters such as the contact radius and stress. Information about the actual shape and dimensions of the tips was obtained from SEM images acquired between the AFAM measurements. Some of the tips tested yielded reproducible values of k^* and showed very little change in shape. Further analysis of the AFAM and SEM results revealed that these tips could withstand stresses much larger than the yield strength of silicon with only minimal wear.

EXPERIMENTAL METHODS

The 12 cantilevers used in this study were commercially available silicon rectangular beams about 240 μm long, 7 μm thick and 35 μm wide. They were randomly chosen from three different sets purchased from the same vendor. Each cantilever was subjected to the same sequence of AFAM measurements, which contained seven separate measurement "tests." Each test comprised measurements at three to six different cantilever deflection δ. In the first test, δ = 10, 20 and 30 nm. The next two tests consisted of measurements at four deflections increasing from 10 nm to 40 nm. In the fourth to seventh tests, δ was increased from 20 nm to 125 nm in six steps. This sequence of tests was chosen in order to investigate the behavior of new tips under progressively higher static loads. The static loads F applied to the tips were calculated from Hooke's law $F = k_c \delta$, where k_c is the cantilever spring constant. The values of k_c ranged from 35 N/m to 42 N/m and were determined for each cantilever individually, as described in detail in Ref. 6. Because the values of F as well as the absolute values of k^* and stresses are dependent on k_c, they have the uncertainty of 5 % that was calculated for k_c.

Tests were performed on a fused quartz sample with ten of the cantilevers. A value $M_{fq} = 68 \pm 2$ GPa for the indentation modulus of the fused quartz specimen was determined by nanoindentation. Additional tests were performed on nickel and sapphire single-crystal samples with two of the cantilevers. Based on pulse-echo ultrasonic measurements and literature values of the elastic constants of single-crystal nickel, the value $M_{Ni<100>} = 219$ GPa ± 2 GPa for the <100>-oriented nickel specimen was calculated. The literature values of the elastic constants for single-crystal sapphire were used to calculate a value of $M_{S<101>} = 423$ GPa [7].

SEM images were obtained for each new tip before engaging it in AFAM measurements. After that the SEM images were acquired for each tip intermittently throughout the AFAM measurement sequence. For most of the tips, the SEM images were obtained after the first, third, fifth and seventh test. The SEM images were analyzed with commercial software to measure the radius of curvature R of each tip [5]. The average value of R obtained from ten separate measurements was taken as the value of R. In order to determine if a tip plastically deformed during the AFAM tests, we compared SEM images obtained for the tip before and after the tests. We made conclusions about tip deformations based on changes in the tip width and on the side edges of the tip.

As mentioned in the introduction, the stress applied to the tips during the AFAM measurements can be greater than the theoretical yield strength of silicon and therefore is an important factor influencing the tip wear. The experimental values of k^* obtained from the AFAM measurements [3] were used to calculate the estimated stress σ_{est} applied to the tips during the measurements. The tip-sample contact stiffness $k^* = 2aE^*$, where a is the contact radius and $E^* = (1/M_t + 1/M_s)^{-1}$ is the reduced Young's modulus. E^* depends on the indentation moduli M_t of the tip and M_s of the sample. The Hertzian model for contact mechanics defines the stress exerted on a half space by a hemispherical tip as [4]:

$$\sigma_{est} = -\frac{3F}{2\pi a^2}. \qquad (1)$$

We compared the values of σ_{est} obtained for our experiments from Eq. (1) to the theoretical value of 5 GPa calculated for the yield strength of single-crystal silicon [5].

RESULTS AND DISCUSSION

The AFM tips used in this study can be divided into two groups: tips that showed extensive changes in their dimensions due to fracture and/or deformation, and tips that did not change. In the first group, the new tips had either $R < 10$ nm or $R > 40$ nm. Figure 1(a) shows an SEM image of an AFM tip with $R < 10$ nm. All four tips with $R < 10$ nm fractured. The tip shown in Fig. 1(a) fractured during the first AFAM test. The abrupt change in the tip radius caused a sudden increase in the values of the measured resonant frequencies. From the values of k^* obtained during the test, we calculated that the fracture occurred at $\sigma_{est} = 30$ GPa. The SEM images obtained after this test verified the fracture and showed that the tip radius had increased to 20 nm. We did not observe further fracture events for this tip. However, during successive tests, we observed a slow increase in k^*, indicating a slow growth in R. The maximum values of σ_{est} decreased after the fracture to 20 GPa and continued to decrease to 15 GPa as the tip radius increased during the subsequent AFAM tests. Figure 1(b) shows an SEM image obtained for this tip after the last AFAM test. The tip radius increased from less than 10 nm to 37 nm. By comparing the images presented in Figs. 1(a) and (b), one can see that the end part of the tip became wider. There is also a slight increase in thickness of the previously sharp edge of the tip, indicating plastic deformation of the tip.

Another example of a tip that plastically deformed in AFAM experiments is presented in Figs. 1(c) and (d). Figure 1(c) shows an SEM image of an AFM tip that was blunt, even when new. Due to the irregular geometry of the tip, it was difficult to determine R. The values of k^* obtained with this tip increased during the AFAM tests, suggesting an

increase in contact radius; however, we did not observe any fracture events. On the other hand, SEM images acquired for this tip showed progressive plastic deformation that occurred at values of σ_{est} ranging from 6 GPa to 7 GPa. An SEM image presenting the state of the tip after the last AFAM test is shown in Fig. 1(d). The tip end became wider, and one can see fold-like structures at the edges of the tip. Similar behavior was observed for two additional tips with initial radii of about 40 nm.

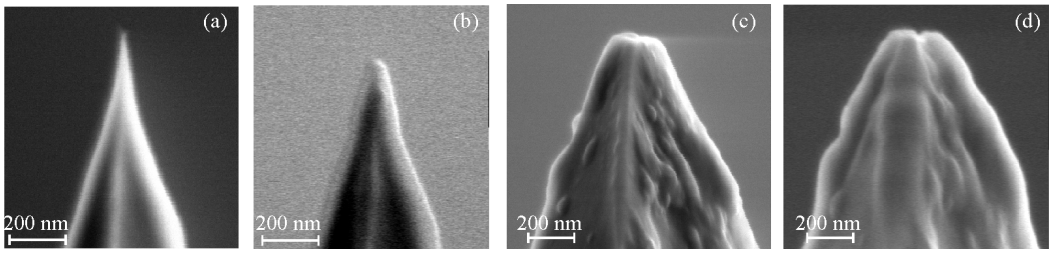

Figure 1. SEM images of tips whose shapes changed during the AFAM tests. (a) SEM image of a new tip with $R < 10$ nm. (b) SEM images of the same tip obtained after the tests shows a fractured and deformed tip with $R = 37$ nm. SEM images of (c) a blunt new tip and (d) the same tip after AFAM tests.

AFM tips that did not change their geometry during the AFAM tests had initial R ranging from 25 nm to 30 nm. Figure 2(a) shows an SEM image of such a tip that was used in a set of AFAM tests on fused quartz. The values of k^* obtained during the tests were reproducible; that is, they changed very little from one test to the next. Such behavior indicates very little tip wear, which is the kind of performance that is desired in AFAM experiments. An SEM image obtained for this tip after the last AFAM test is shown in Fig. 2(b). Comparison of Figs. 2(a) and (b) reveals that the tip shape had not changed, except for a relatively small increase in R from 25 nm to 30 nm. Two additional tips with similar values of R also performed very well when tested on fused quartz.

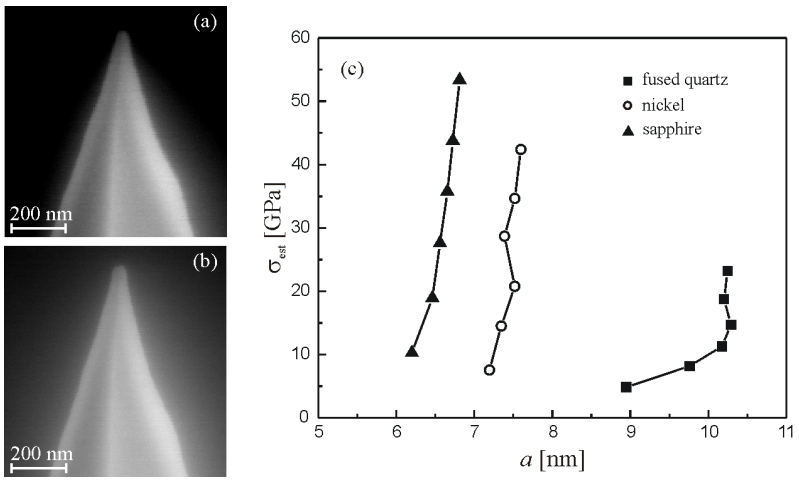

Figure 2. (a) SEM image of a new AFM tip with $R = 25$ nm. (b) The same tip with $R =$ 30 nm after the AFAM tests. (c) Comparison of stress σ_{est} as a function of contact radius a calculated for tips used in AFAM experiments on fused quartz, nickel and sapphire. The applied static loads ranged from 0.4 μN to 6 μN.

In order to further test the performance of this kind of tip, we tested two more tips with $R = 25 – 30$ nm on the nickel and sapphire samples. SEM images obtained for these tips also showed no significant changes in their shape and dimensions. From the values of k^* obtained on all three materials, we calculated values for a and the corresponding σ_{est}. The results are presented in Fig. 2(c). As can be seen in the figure, the values of a are below 11 nm. This means that even for tips with $R \approx 30$ nm, material properties can be probed with high spatial resolution. The maximum values of σ_{est} applied during the tests increased with the modulus of the sample from 25 GPa to 50 GPa, five to ten times greater than the theoretical yield strength of bulk silicon. Because no visible plastic deformation was observed in the SEM images, we concluded that AFM tips with an initial R of 25nm to 30 nm exhibited a good combination of yield and fracture strength.

The enhanced strength observed for tips with $R \approx 30$ nm in comparison to that for tips with $R > 40$ nm agrees with the quantitative results of size-effect studies published by other groups. Gerberich *et al.* found that silicon nanospheres displayed hardness that was greater than that of bulk material and inversely proportional to the radius of the spheres [8]. Greer *et al*. showed that the yield strength of freestanding pillars of single-crystal gold increased with decreasing diameter [9]. These studies agreed that "smaller is stronger", but proposed different theories to explain the observed size effects. The increased hardness of the silicon nanospheres was explained by the presence of hypothetical dislocation loops that nucleated at the top and the bottom of the compressed sphere and moved up and down in a glide cylinder [8]. The theory proposed for gold pillars [9] claimed that within a small volume, dislocations were not able to multiply and that plastic deformation could not occur due to dislocation starvation.

However, if smaller is stronger, why did our tips with $R < 10$ nm fracture? We are not aware of any size-effect studies on freestanding structures as small as our sharpest tips. Because our studies were not originally designed to study size effects, we can consider only the specifics of our system. In AFM systems, the tip approaches the sample surface at an angle of 11º to 15º. Unlike the experimental conditions reported in Refs. 8 and 9, the resulting stress is not uniaxial and has shear and bending components. Therefore, in our experiments the shear strength and fracture toughness of the tip should be considered as well. In addition, an AFM silicon tip has a native silicon oxide layer. Assuming a thickness of 1 nm to 2 nm for the oxide layer, the resulting volume ratio of silicon oxide to silicon can be significant for very sharp tips. As a consequence, the structure may be weaker and more prone to fracture in the shear direction. One may also look for an analogy between these single nanocrystals and nanocrystalline materials, and say that small structures become stronger only until they reach an optimal size, as observed previously in nanocrystalline metals [10].

SUMMARY AND CONCLUSIONS

We have studied the changes in shape that occurred during a series of defined AFAM experiments with 12 tips. The tips were used in contact mode at increasing static loads. Information about the changes induced in the tips' shape, such as increase in R, fracture, and plastic deformation, was obtained from high-resolution SEM images that were

acquired between the individual tests. Values of the contact stiffness k^* obtained in the AFAM tests were used to determine the tip-sample contact radius a and stress σ_{est}. Based on the analysis of the AFAM results and SEM images, we divided the tips into two groups: tips whose shape changed due to fracture and/or plastic deformation, and tips whose form was preserved during the whole set of AFAM tests. Tips with $R > 40$ nm deformed plastically. Qualitative analysis of the SEM images and values of σ_{est} calculated from the experimental values of k^* suggested that for the larger tips, the maximum values of σ_{est} to deform the tip are comparable with the theoretical yield strength of silicon. Tips with $R < 10$ nm also changed due to fracture and plastic deformation, but they fractured at relatively large stress (30 GPa). Tips that displayed the best performance, that is, yielded reproducible values of k^* during subsequent AFAM tests, had R ranging from 25 nm to 30 nm. No significant changes in the shape of these tips were observed in the SEM images, even after stresses σ_{est} greater than 30 GPa.

Our results indicate that most of the silicon tips used in AFAM experiments were stronger than bulk silicon, because they showed increased resistance to deformation and fracture. However, the strength depended on the initial size of the tip. The tips became stronger as R decreased to 25 nm to 30 nm; however, tips with $R < 10$ nm fractured on a regular basis. The size effects observed for these tips may prove beneficial for AFM-based techniques. In our test group of twelve AFM tips, we found five with $R = 25$ nm to 30 nm, which appears optimal for both lateral resolution and durability. These optimal tips endured stresses ten times greater than the theoretical yield strength of bulk silicon without plastic deformation or fracture while in contact with samples that were up to 2.5 times stiffer than silicon. These results suggest that the problem of tip wear, which is one of the greatest sources of uncertainty in the AFAM method, can be greatly reduced by optimizing the tip radius. Using silicon tips with optimized tip radius may allow us to preserve the simplicity of the AFAM experimental approach and data analysis model, while ensuring reproducible and reliable measurements.

REFERENCES

1. K. Yamanaka, A. Noguchi, T. Tsuji, T. Koike, and T. Goto, *Surf. Inter. Anal.* **27,** 600 (1999).
2. M. T. Cuberes, H. E. Assender, G. A. D. Briggs, and O. L. Kolosov, *J. Phys. D: Appl. Phys.* **33,** 2347 (2000).
3. U. Rabe *et al.*, *Ultrasonics* **38,** 430 (2000).
4. K. L. Johnson, *Contact Mechanics* (Cambridge University Press, Cambridge UK, 1985) p. 92.
5. A. L. Ruoff, *J. Appl. Phys.* **50**, 3354 (1979).
6. M. Kopycinska-Müller, R. H. Geiss, and D. C. Hurley, *Ultramicroscopy* 2006, in print.
7. G. Simmons and H. Wang, *Single crystal elastic constants and calculated aggregate properties: A handbook* (The MIT Press, Cambridge, MA, 1971) p.56.
8. W. W. Gerberich *et al.*, *J. Mech. Phys. Solids* **51**, 979 (2003).
9. J. R. Greer, W. C. Oliver, and W. D. Nix, *Acta Mater*. **53**, 1821 (2005).
10. Y. Zhou, U. Erb, K. T. Aust, and G. Palumbo, *Scripta Mater.* **48,** 825 (2003).